

Accreting white dwarf models for CAL 83, CAL 87 and other ultrasoft X-ray sources in the LMC

E.P.J. van den Heuvel^{1,2}, D. Bhattacharya^{1,2,*}, K. Nomoto^{1,3}, and S.A. Rappaport^{1,4}

¹ Institute for Theoretical Physics, University of California, Santa Barbara, CA 93106-4030, USA

² Astronomical Institute “Anton Pannekoek” and Center for High Energy Astrophysics, Kruislaan 403, 1098 SJ Amsterdam, The Netherlands

³ University of Tokyo, Department of Astronomy, Bunkyo-ku, Tokyo 113, Japan

⁴ Department of Physics and Center for Space Research, Massachusetts Institute of Technology, Cambridge, MA 02139, USA

Received August 28, 1991; accepted February 13, 1992

Abstract. It is shown that the ultrasoft X-ray emission (peak energy 30–50 eV) observed in the three strong ($\geq 4 \cdot 10^{37} - 10^{38} \text{ erg s}^{-1}$) LMC X-ray sources CAL 83, CAL 87 and RXJ 0527.8–6954 can be explained by steady nuclear burning of hydrogen accreted onto white dwarfs with masses in the range of 0.7 to $1.2 M_{\odot}$. The observed optical and X-ray characteristics of the binary systems CAL 83 ($P = 1.04^{\text{d}}$) and CAL 87 ($P = 10.6^{\text{h}}$) are shown to be consistent with such a model. In both systems the companions are main-sequence stars with masses in the range of 1.5 to $2 M_{\odot}$. They are transferring mass unstably on a thermal timescale by Roche-lobe overflow, at rates between 1.0 and $4.0 \cdot 10^{-7} M_{\odot} \text{ yr}^{-1}$.

In both systems the white dwarf with its accretion disk is the dominant optical light source, being much brighter than the unheated side of the companion. The donor stars in these systems appear to be strongly heated. We argue that the stellar wind emanating from the heated star interacts with that from the disk (plus white dwarf) to generate the He II 4686 emission line with a radial velocity amplitude much lower than the actual radial velocity amplitude of the white dwarf, thus yielding an apparently much too large mass estimate of this compact star.

We suggest that CAL 83 and CAL 87 are the white dwarf analogues of X-ray binaries like Her X-1. Because the accreted matter in these sources would not be ejected in thermonuclear nova flashes, the white dwarfs in these systems may eventually collapse to form neutron stars.

Key words: X-ray sources – accretion – white dwarfs – neutron stars

1. Introduction

The peak photon energies of the strong ($\geq 4 \cdot 10^{37} - 10^{38} \text{ erg s}^{-1}$, see below) LMC X-ray sources CAL 83 and CAL 87 are some hundred times lower than those of the traditional strong binary X-ray sources.

Send offprint requests to: E.P.J. van den Heuvel

*On leave from Raman Research Institute, Bangalore, India

While the energy distributions of the latter (accreting neutron stars and black holes) peak between 1 and 10 keV, those of the ultrasoft sources peak between 30 and 50 eV, as follows from model simulations for obtaining their observed intensities in the ROSAT energy bands (Trümper et al. 1991; Greiner et al. 1991). ROSAT has discovered a third source of this type, RXJ 0527.8–6954 (Trümper et al. 1991). These observations indicate that these objects form a separate new class of X-ray sources, not previously encountered in our galaxy. Indeed, such sources in the plane of the Galaxy must be within a distance of less than ~ 1 kpc in order to be observable, since at larger distances interstellar absorption will extinguish them.

Extrapolating from the number observed in the LMC, the probability of finding one such source within ~ 1 kpc from the Sun is negligible. The reason why the sources are observable in the LMC is, apparently, the relatively low interstellar column density in the direction of the LMC. CAL 83 and CAL 87 have been optically identified with close binary systems with orbital periods of 1.04 days and 10.6 h, respectively (Smale et al. 1988; Pakull et al. 1988; Cowley et al. 1990). In analogy with the other binary X-ray sources it is therefore very likely that these are accreting binary systems. The striking difference of about a factor 100 in peak X-ray energy relative to the accreting neutron star and black hole binaries strongly suggests that the accreting objects in the ultrasoft sources have radii $\sim 10^2 - 10^4$ times larger than that of a neutron star (10^2 assuming that the temperature is proportional to the potential energy released per unit mass of accreted matter, and 10^4 assuming a scaling according to Stefan–Boltzmann law for a fixed luminosity), i.e. characteristic of a white dwarf.

The existing suggestions regarding the nature of these sources include accreting black holes (Cowley et al. 1990; Smale et al. 1988) and neutron stars accreting matter at or above Eddington rate (Greiner et al. 1991). There are, however, serious doubts as to whether spectra as soft as those seen in Cal 83, Cal 87, or RXJ 0527.8–6954 can in fact be produced by accreting neutron stars or black holes. The known black hole candidates such as Cyg X-1 and LMC X-3 exhibit softer X-ray spectra than typical neutron star sources, but their characteristic temperatures are still in the keV range, much higher than the supersoft LMC sources. It has been argued by Greiner et al. (1991) that as the mass transfer

rate onto a neutron star increases, its X-ray spectrum would get progressively softer, since the cocoon of matter surrounding the accreting object would cause the photospheric radius to expand. The X-ray source Cen X-3, believed to be a neutron star accreting close to the Eddington limit appears to behave differently, however (Giacconi 1975). The X-ray spectrum becomes progressively harder with increasing accretion rate, until the X-rays are completely quenched at mass accretion rates that are above the Eddington rate. Quenching appears when the column density between us and the source exceeds $\sim 0.5 \text{ g cm}^{-2}$. LMC X-4, on the other hand, goes up to ~ 20 times the Eddington luminosity and becomes softer, but still the effective temperature remains of order a few keV (Levine et al. 1991). In a super Eddington situation a quenching column-density is expected to always ensue at a high enough accretion rate which the neutron star is unable to accept. The excess matter will pile up around the source, causing the column density to increase, until it exceeds 0.5 g cm^{-2} and the source is quenched. The quenching is due to the fact that the major source of X-ray opacity is the photoionization of the surrounding matter. If the accretion rate is too large the X-ray photon flux is too low to keep all the incoming matter ionized. The recombination rate in a dense ionized gas is sufficiently high once $L_x/(n_e r^2)$ (L_x =X-ray luminosity of the source, n_e =the electron density, r =distance from the central source) is sufficiently low, causing the X-rays to be degraded into mainly optical and UV radiation. No special processes are known that would favour the transformation of the hard X-ray flux into a 30–50 eV blackbody, as seems to be the case here (see Hatchett & McCray 1977).

A further problem with the interpretation of these sources as super-Eddington accreting neutron stars is the following. Mass transfer rates well above the Eddington limit can be obtained in systems where the donor mass exceeds $\sim 1.4 M_\odot$. The duration of this phase, and consequently the probability of observation decreases rapidly with increasing donor mass. As a result, the most promising neutron star systems would be those where the donor mass lies between 1.4 and $2 M_\odot$. The optical properties of the systems CAL 83 and CAL 87 also do not allow donor masses higher than this (see Sects. 4 and 5). The X-ray binary Her X-1 would be an ideal progenitor of this phase. The present sub-Eddington accretion phase in Her X-1 is expected to last $\lesssim 4 \times 10^5$ yr (Savonije 1983), while the super-Eddington phase is expected to last $\sim 10^7$ yr. Given the fact that we see one Her X-1, this would indicate that there are at least 25 systems in our galaxy in the post-Her X-1 phase. These systems are expected to receive large ($\sim 100 \text{ km s}^{-1}$) centre-of-mass velocities when the neutron star is born, as can be clearly seen from the fact that Her X-1 is situated 3 kpc above the galactic plane. Such velocities would make the distribution of these super-Eddington sources very wide, with a scale height of order a kpc. With such a wide distribution, many systems are expected to lie outside the obscuring interstellar matter in the galaxy, and would surely have been observed with earlier X-ray satellites had they been such bright soft X-ray sources as have been observed in the LMC. This leads us to conclude that apparently the cocoons around neutron stars undergoing super-Eddington accretion grow so large as to reprocess the radiation to much longer wavelengths, and are unlikely to explain the large soft X-ray luminosities observed from CAL 83, CAL 87, and RXJ 0527.8–6954.

Given these difficulties with the neutron star/black hole model for the supersoft sources, we explore in this paper the possibility

that the accreting objects in these systems may be white dwarfs. We find that a reasonable explanation for the observed properties of these sources can be provided by such a hypothesis.

In Sect. 2 we explore the conditions under which an accreting white dwarf may reach an X-ray luminosity and effective temperature similar to those observed for the supersoft LMC sources.

We show that there is a range of white dwarf masses and (hydrogen) accretion rates for which such sources can be produced. The required white dwarf masses and accretion rates are $0.7\text{--}1.4 M_\odot$ and $\sim 1\text{--}5 \times 10^{-7} M_\odot \text{ yr}^{-1}$, respectively. Such accreting white dwarf models appear to fit the observed optical and X-ray properties of CAL 83 and CAL 87. In CAL 87 the companion star is a main-sequence star of mass $\sim 1.4\text{--}1.5 M_\odot$, in CAL 83 it is most probably a post-main-sequence star with a mass in the range $1.5\text{--}2 M_\odot$. The theoretically derived mass-transfer rates by Roche-lobe overflow for these companion masses are $\sim 10^{-7} M_\odot \text{ yr}^{-1}$ and $\sim 4 \times 10^{-7} M_\odot \text{ yr}^{-1}$, respectively, and the inferred X-ray lifetimes of the systems are $\sim 10^7$ yrs.

In Sect. 6 we discuss the possible evolutionary origins and the fate of these accreting white dwarf binaries.

2. Origin of the X-ray spectrum: the nature of the accreting white dwarfs

As we remarked above, the X-ray spectra of CAL 83, CAL 87, and RXJ 0527.8–6954 are unusually soft. From the ROSAT observations of CAL 83 and RXJ 0527.8–6954 a blackbody temperature $kT_{\text{bb}} < 50$ eV is indicated for these sources (Trümper et al. 1991; Greiner et al. 1991). According to the spectral hardness ratios obtained from Einstein IPC observations (Long et al. 1981), the spectrum of CAL 87 is somewhat harder than that of CAL 83, but would still be characterized by $kT_{\text{bb}} < 100$ eV. CAL 83 is the brightest among these three sources, having a count rate ~ 4 times larger in the IPC band than CAL 87, and ~ 3.5 times that of RXJ 0527.8–6954 in the ROSAT PSPC (Greiner et al. 1991). Greiner et al. (1991) present blackbody fits for CAL 83 and RXJ 0527.8–6954 for different values of N_{H} . While the best fit values for kT_{bb} and N_{H} indicate luminosities $L_{\text{bb}} \sim 10^{40} \text{ erg s}^{-1}$ for these sources, the uncertainties in these parameters are rather large, and the 99% confidence limits include L_{bb} values as low as $10^{37} \text{ erg s}^{-1}$ (Fig. 1). For the canonical value of $N_{\text{H}} \sim 7 \times 10^{20} \text{ cm}^{-2}$ in the line of sight to the LMC the luminosities turn out to be $\sim 7 \times 10^{37} \text{ erg s}^{-1}$ and $\sim (3\text{--}20) \times 10^{37} \text{ erg s}^{-1}$ for Cal 83 and RXJ 0527.8–6954, respectively.

An accreting white dwarf undergoes nuclear burning when the accretion rate exceeds a certain limit. Then the stellar luminosity is dominated by hydrogen burning, since the energy liberated by hydrogen burning exceeds that due to accretion on a white dwarf by an order of magnitude or more, depending on the mass of the white dwarf. It has been shown by Nomoto et al. (1979) and Sienkewicz (1980) that above an accretion rate (with a hydrogen abundance of 0.7 by mass) $\dot{M}_{\text{RG}} \approx 8.5 \times 10^{-7} (M_{\text{WD}}/M_\odot - 0.52) M_\odot \text{ yr}^{-1}$ (M_{WD} =mass of the white dwarf) the accreted matter forms a red-giant like envelope around the white dwarf, with the luminosity being generated from hydrogen shell burning. Steady hydrogen burning on the white dwarf surface can occur for $0.4 \dot{M}_{\text{RG}} \lesssim \dot{M} \lesssim \dot{M}_{\text{RG}}$ (Paczynski & Żytkow 1978; Sion et al. 1979; Sienkewicz 1980), processing hydrogen into helium at the rate of accretion. At lower accretion rates, hydrogen burning is unstable and occurs in flashes, with only the much lower accretion luminosity visible from the white dwarf in between flashes.

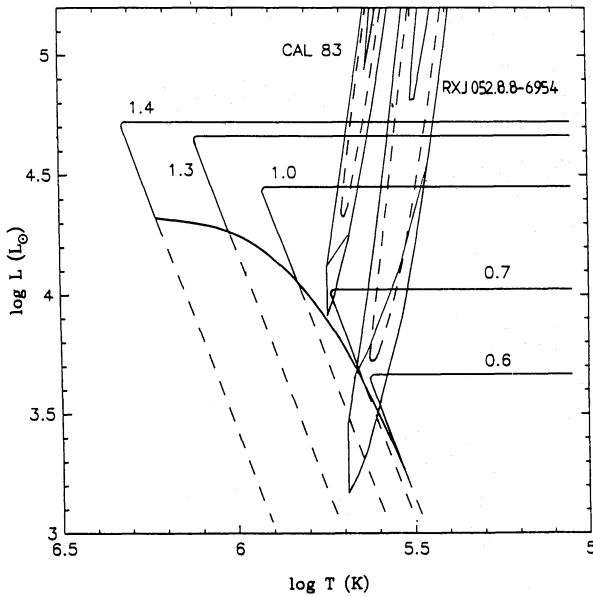


Fig. 1. Hertzsprung–Russell diagram for accreting white dwarfs with steady (stable or unstable) nuclear burning on the surface. Curves are labelled with the corresponding masses of the white dwarfs (in solar masses). The almost horizontal portions of the tracks correspond to \dot{M} for which the accreted envelope around the white dwarf expands to form an extended structure. The extreme case of a red-giant envelope corresponds to a maximum luminosity L_{RG} for each white dwarf mass. Steady nuclear burning on the white dwarf is stable between $0.4L_{\text{RG}}$ and L_{RG} . These portions of the tracks are indicated by solid straight lines. In the region indicated by dashed straight lines, the steady burning solution is unstable and burning thus occurs in flashes. Locations of the two ultrasoft sources, CAL 83 and RXJ 0527.8–6954, in the total luminosity–temperature plane are indicated by contours of 68% (solid, inner), 95% (dashed) and 99% (solid, outer) confidence levels corresponding to those published by Greiner et al. (1991). The thin sloping lines across the contours correspond to the “canonical” N_{H} value of $7 \cdot 10^{20}$ along the line of sight to the LMC

The luminosity corresponding to the above lower limit for stable hydrogen burning, $0.4L_{\text{RG}}$, is indicated by the solid curve in Fig. 1. In Fig. 2 this lower limit and the corresponding luminosity is indicated for various values of the white dwarf mass. Figure 1 is based on the calculations by Nomoto (1982) and Sienkiewicz (1980) and shows the temperatures and luminosities generated in the regime of steady hydrogen burning. The almost horizontal portions of the tracks represent the formation of a highly distended red-giant envelope and the consequent drop in the effective temperature as \dot{M} gets close to \dot{M}_{RG} . On the same diagram are shown the estimated positions of the LMC sources Cal 83 and RXJ 0527.8–6954, as error ellipses of 68%, 95% and 99% confidence level obtained from blackbody fits to the ROSAT observations (Greiner et al. 1991). Values corresponding to the “canonical” $N_{\text{H}} \sim 7 \cdot 10^{20} \text{ cm}^{-2}$ along the line of sight to the LMC are also indicated in the diagram. As is clear from Fig. 1, spectra consistent with those observed can be produced by accreting white dwarfs only if \dot{M} is close to or larger than \dot{M}_{RG} . The required mass of the white dwarf is $\geq 0.7M_{\odot}$ for RXJ 0527.8–6954 and above $\geq 0.8M_{\odot}$ for Cal 83, with corresponding accretion rates $\geq 1.5 \cdot 10^{-7} M_{\odot} \text{ yr}^{-1}$ and $\geq 2.4 \cdot 10^{-7} M_{\odot} \text{ yr}^{-1}$, respectively.

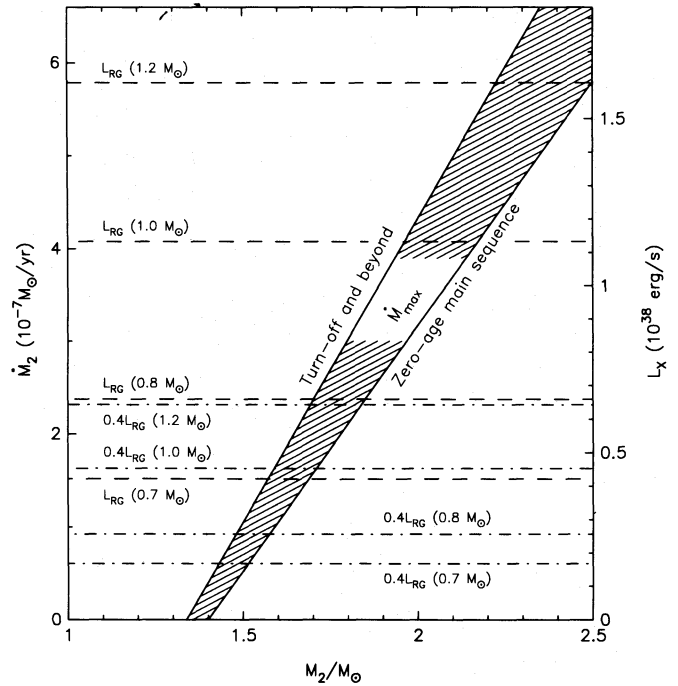


Fig. 2. Mass-transfer rate \dot{M}_2 as a function of companion mass M_2 for systems consisting of a main-sequence star (mass M_2) and a less massive compact star, as calculated by Pylyser & Savonije (1988, 1989). At a given mass M_2 , the lowest \dot{M}_2 values occur for companions of zero age main sequence, and the highest values for companions near turn-off of the main sequence and beyond. Also indicated (on the right-hand side) are the corresponding luminosities produced by nuclear burning and accretion on white dwarfs in such systems. The dashed (dash-dotted) horizontal lines indicate maximum (minimum) possible steady X-ray luminosities L_{RG} that can be produced by nuclear burning on accreting white dwarfs, of masses $0.7M_{\odot}$, $0.8M_{\odot}$, $1.0M_{\odot}$ and $1.2M_{\odot}$.

3. The possible occurrence of a “limit cycle” behaviour at $\dot{M} > \dot{M}_{\text{RG}}$

As can be seen from Fig. 1, the characteristic temperature of the emergent spectrum is highly sensitive to the accretion rate when $\dot{M} \approx \dot{M}_{\text{RG}}$. The difference in \dot{M} between the hottest and the coolest parts of the horizontal track in Fig. 1 is only $\sim 10\%$. If indeed $\dot{M} \approx \dot{M}_{\text{RG}}$, the spectrum is expected to undergo considerable variations in detectable soft X-ray luminosities for small changes in \dot{M} . In particular, if the temperature falls below $\sim 10^5$ K, the sources would become virtually unobservable in X-rays. This may explain the non-detection of RXJ 0527.8–6954 by the Einstein observatory.

In tight binary systems such as Cal 83 and Cal 87 the envelope of the accreting white dwarf cannot, however, expand without bounds. As the size of the envelope grows beyond the Roche lobe, it is likely to prevent further mass flow towards the white dwarf. As a result, a limit cycle of the following nature will probably develop.

As matter arrives at a rate $\dot{M} > \dot{M}_{\text{RG}}$ on the white dwarf, hydrogen burning is ignited and generates a luminosity as high as L_{RG} (i.e. the horizontal line in Fig. 1). As the accumulated mass increases, the accreting star would begin to grow in photospheric radius, and its temperature would drop significantly (Nomoto et al. 1979). Once the “giant” configuration fills its Roche lobe,

any further matter transferred from the donor star would probably be ejected from the system, via the second Lagrangian point. The donor star is at this stage surrounded by the outer parts of the giant envelope. The mass ($\sim 10^{-5} M_{\odot}$) and hence the density of this envelope is so small that no spiral-in will occur before the available nuclear fuel on the white dwarf has been exhausted in ~ 100 yr [see Eq. (10) of Nomoto 1982]. The hydrogen shell burning will then stop, and cause the envelope to collapse. This would allow mass flow to the white dwarf to recommence and the cycle to begin again.

The radius R_G of the developing giant in the phase of expansion can be shown to behave as $\log R_G \propto \Delta M$, where $\Delta M = \dot{M}\Delta t$ is the amount of accumulated fuel (Nomoto et al. 1979). Thus, the radius as a function of time after the cycle starts is given simply by

$$R_G = R_0 e^{\dot{M}\Delta t/\Delta M_0} \quad (1)$$

where R_0 is the original white dwarf radius and ΔM_0 is the accumulated envelope mass required for an e-fold increase in radius. For a fixed luminosity generated by hydrogen shell burning, the temperature T scales as $R^{-1/2}$, and its time behaviour can therefore be written as

$$T = T_{\max} e^{-\dot{M}\Delta t/2\Delta M_0} \quad (2)$$

This expression shows that the time spent by the star at $0.8T_{\max} < T < T_{\max}$ is $\sim 10\%$ that at $0.1T_{\max} < T < 0.8T_{\max}$, suggesting that the source would be “on” in soft X-rays for at least 10% of the time.

We note that the dynamics of mass being transferred into the envelope of a giant and the subsequent temporal evolution of the expanding envelope need to be computed quantitatively before the details of a possible limit-cycle behaviour scenario can be understood.

The existence of an emission nebula around Cal 83 indicates that considerable mass loss from the system has taken place in the past. This would fit with the mass-loss episodes from the system expected from a limit-cycle behaviour as described above.

4. Companion masses required for the accreting white dwarf models

Mass transfer rates in the range $(1-4)10^{-7} M_{\odot} \text{ yr}^{-1}$, as are required for transforming accreting white dwarfs into near-Eddington-limited supersoft X-ray sources, can be obtained in short-period binaries ($P \lesssim 1-2^d$) by Roche-Lobe overflow mass transfer from a companion that is more massive than the white dwarf (Paczynski 1971; Savonije 1983). In such a case, the mass transfer is secularly unstable (since the system shrinks as mass is being transferred) and takes place on a timescale of order of the thermal timescale of the donor star. Evolution of similar systems have been computed in detail by Pylyser & Savonije (1988, 1989). Their results show that \dot{M} just in the above range occur in systems with donor masses between $1.5M_{\odot}$ and $2M_{\odot}$. According to these calculations, the resulting mass-transfer rates depend mainly on the mass and the evolutionary state of the donor, and only slightly on the mass of the accreting star (for accretors in the mass range $0.7M_{\odot}$ to $1.3M_{\odot}$). Figure 2 represents the mass accretion rates, \dot{M}_2 , as a function of the mass M_2 of the donor, for donors on the

zero-age main sequence (ZAMS) and near core-hydrogen exhaustion (“turn-off”). For the few systems calculated with post-main sequence donors, the \dot{M} values were close to the values for “turn-off” donors.

Therefore, one expects the mass transfer rates \dot{M}_2 as a function of M_2 to be located in the hatched band in Fig. 2.

The figure shows that, if one assumes the masses of the white dwarfs to be $\geq 0.7M_{\odot}$ stable hydrogen burning can be achieved only for $M_2 \geq 1.45M_{\odot}$. On the other hand, for M_2 in the range $2.0-2.2M_{\odot}$ the accretion rate exceeds the one required to power an Eddington-limited source with a $1.2M_{\odot}$ white dwarf. Since no white dwarfs more massive than this value are known, the required companion masses should not exceed $2.2M_{\odot}$.

It thus appears that companion stars in the mass range $1.4M_{\odot}$ to $2.2M_{\odot}$ are the ones required for turning white dwarfs with masses between $0.7M_{\odot}$ and $1.2M_{\odot}$ in short-period binaries ($P \lesssim 1-2$ days) into near-Eddington limited supersoft X-ray sources.

Such companion masses appear to be just the ones that excellently fit the observed optical characteristics of the well studied systems Cal 87 and Cal 83, as we shall now show.

5. The optical light and radial velocity curves of CAL 87 and CAL 83, and the accreting white dwarf model

5.1. Introduction

CAL 87 was optically identified with a 18^m9 star in the LMC by Pakull et al. (1988). It shows the very blue continuum and He II 4686 emission line characteristic of low-mass X-ray binaries, in which the dominant light source is an accretion disk (see e.g. Bradt & McClintock 1983; van Paradijs 1983). The same holds for CAL 83, which was identified with a 16.96 magnitude star in the LMC by Smale et al. (1988). As in other low-mass X-ray binaries in the LMC, the Bowen-excited N III/C III complex near $\lambda 4640$ in both systems is much weaker than in galactic low-mass X-ray binaries, presumably due to the low heavy-element abundance of the LMC.

Both systems were found to be binaries though, at first glance, with very different optical lightcurves, as schematically depicted in Fig. 3. The orbital period of 10.6^h of CAL 87 was discovered by Naylor et al. (1989; see Callanan et al. 1989) and confirmed by Cowley et al. (1990). The optical photometric period of 1.04 days of CAL 83 was discovered by Smale et al. (1988), as a result of a world-wide observing campaign in 1983-1985.

The fact that in both systems the H α line is in emission (see e.g. Pakull et al. 1988) shows that the mass-donor star in both systems is hydrogen rich.

In view of the apparently very different optical lightcurves of the two systems, we will now discuss each system separately, but later on will proceed to show that the systems are, in fact quite similar – differing only in orbital inclination and (slightly) in companion mass.

5.2. The CAL 87 system

5.2.1. Constraints imposed by the light curve

The optical lightcurve of the system (Fig. 3a) looks reminiscent of a classical eclipsing binary, showing one deep (primary) minimum (1^m2) at phase 0.0, lasting about 0.45 in phase from ingress to egress, and a shallow (0^m2 on average, but sometimes up to 0^m4)

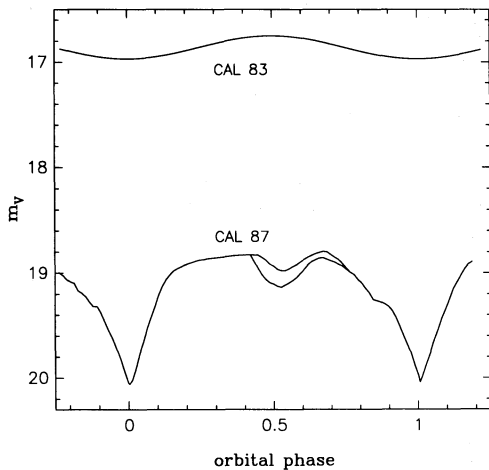


Fig. 3. Schematic light curves of CAL 83 (top) and CAL 87 (bottom) plotted on the same scale for comparison. The two different curves near the secondary eclipse of CAL 87 correspond to the range of variations observed in this region of the light curve (see Cowley et al. 1990)

secondary minimum, slightly displaced with respect to phase 0.5 (Cowley et al. 1990) and lasting ~ 0.20 in phase. We note, however, that the primary eclipse is too wide to be explained by two mutually occulting objects contained within their respective Roche lobes. In fact, the maximum eclipse duration for two Roche-lobe-filling objects (with mass ratio less extreme than 10:1) viewed in the orbital plane should be ~ 0.28 in orbital phase (i.e. $\sim 100^\circ$).

At primary minimum the visual magnitude is $V \approx 20^m1$, and the system is about 0.15 magnitudes redder in $B - V$ than at other phases. Only during primary minimum (phases 0.9 to 0.1) does the spectrum of a star, of spectral type between F5 and early G, become detectable (Cowley et al. 1990). At other phases the spectrum is completely dominated by a strong blue continuum plus the few strong emission lines characteristic of an accretion disk. Since part of the latter light is also still present during the primary minimum, the spectral type of the companion is not well determined (Cowley et al. 1990). (We caution, however, that there is a small but non-negligible probability that the F or G star may simply be a chance superposition with the CAL 87 system.) The fact that the primary minimum has no flat bottom indicates that the primary eclipse is not total, i.e. that part of the light of the disk is still present during this phase.

The model that emerges from the above summary of the photometric and spectroscopic behavior of the system is that of an X-ray illuminated region (including an accretion disk and the heated surface of the secondary) whose reprocessed light accounts for $\sim 80\%$ of the light of the system, together with a normal F or early G-type main-sequence star whose unheated (intrinsic) luminosity provides the remaining portion ($< 20\%$) of the system's light. During the primary minimum most of the X-ray illuminated region is eclipsed by the (relatively dark) secondary; during the secondary minimum the accretion disk eclipses a part of the companion star.

The observed orbital period of 10.6 h for this system imposes a constraint on the mass, M_2 , and radius, R_2 , of the secondary such that $(R/R_\odot)^3(M_\odot/M) < 1.39$ in order that the secondary fit within its Roche lobe. This condition is satisfied for main-sequence stars that are later than spectral type F3 for which $M_2 \approx 1.5M_\odot$ and

$R_2 \approx 1.3R_\odot$. This is indeed consistent with the range of spectral types suggested by Cowley et al. (1990).

We estimate from the light curve that at maximum brightness the apparent visual magnitude is $V \sim 18.8$. If we use the known distance modulus for the LMC of $\sim 18^m4$, and adopt a typical value of $A_V \sim 0^m4$ for the visual extinction, we find that at maximum brightness, the system has $M_V \sim 0.0$. In this case, an unheated F3 main-sequence star is expected to contribute no more than $\sim 5\%$ of the light during the bright portions of the light curve and, therefore, even a complete eclipse of such a star by the accretion disk should be no deeper than $\sim 0^m05$. Moreover, if $2/3$ of the reprocessed light of the system is eclipsed during the primary minimum (to explain the depth 1^m2) the intrinsic light of an F3 star is only very marginally sufficient ($\sim 15\%$ of the total light) to be detectable at primary minimum.

In summary, there are two principal difficulties with the interpretation of the observed light curve in terms of a primary minimum due to the partial eclipse of the accretion disk by the companion star and a secondary minimum due to the eclipse of an unheated F or G-type companion star by the accretion disk. These are (1) the extremely large width of the primary eclipse and (2) the large and variable depth of the secondary minimum. The depth of the secondary minimum can easily be enhanced by invoking X-ray heating of the companion star but then, as noted by Cowley et al. (1990), the shape of the lightcurve just before and after this minimum should be considerably more rounded (e.g. 4U2129+47; McClintock et al. 1981) than is observed. This problem may be alleviated to some degree by assuming that the companion star is *not* corotating with the orbit and may therefore experience X-ray heating more uniformly around its equator. Moreover, since the variable depth of the secondary eclipse is apparently not accompanied by corresponding changes in the brightness during the flat portion of the lightcurve preceding and following the secondary minimum, this implies that it is the size and/or projected shape of the occulting portion of the accretion disk that is variable. The solution to the problematic wide primary eclipse may be found by invoking a strong stellar wind emanating from the companion star due to the X-ray heating. Such a wind would have to be optically thick to light out to a distance from the center of the companion star equal to $\sim 1.4R_2$ on the ingress side of eclipse and $\sim 1.2R_2$ on the egress side (to match the asymmetric shape of the primary eclipse). The sense of this asymmetry is consistent with the expected flow pattern of a stellar wind which is strongly influenced by coriolis forces.

Our current understanding of the physical conditions in the Cal 87 system are insufficient to allow detailed modelling of the optical lightcurve at the present time. We see nothing, however, in the lightcurve to favor its interpretation in terms of a massive black hole as the accreting object. In particular, such an assumption does not help to explain the very wide primary minimum. For example, in a system with a $20M_\odot$ black hole accretor, a $1.5M_\odot$ companion star can be in position to occult some portion of the accretion disk for no more than ~ 0.29 in orbital phase.

Finally, in this regard, we note that only a modest amount of X-ray heating is required to explain either the depth of the secondary minimum or the brightness of the inferred accretion disk. We estimate that all the light at maximum brightness amounts to an optical luminosity of $\lesssim 10^{36} \text{ erg s}^{-1}$ (for an assumed bolometric correction of $< 0^m4$). Even if all of this light

has an origin in X-ray illuminated matter, this requires an X-ray luminosity of $\lesssim 10^{38}$ erg s $^{-1}$ for a conversion efficiency (from X-radiation to optical) of 1%. If CAL 87 is detected as an ultrasoft X-ray source by ROSAT, it will be interesting, therefore, to see if super-Eddington luminosities are inferred, as is the case for CAL 83 and RX J0527.8–6954 (Greiner et al. 1991).

5.2.2. Radial velocity curve and variability of the He II 4686 line

Cowley et al. (1990) find that the He II 4686 line has a full-width at half maximum of 16 Å, corresponding to 1050 km s $^{-1}$. At zero intensity (continuum level) its width is 2100 km s $^{-1}$.

In view of this width Cowley et al. (1990) notice that accurate radial velocities are difficult to determine. The “radial velocities” obtained by line-fitting appear to vary roughly with an amplitude $K \approx 40$ km s $^{-1}$, though with much scatter. The *phase* of the radial-velocity curve relative to the eclipsing binary lightcurve is consistent with that of the orbital motion of the accretion disk of the compact star. Or, more generally, it is consistent with the orbital motion of a point on the line connecting the compact star and the center of mass of the system.

Cowley et al. (1990) argue that the radial velocity of the He II 4686 line represents the radial velocity of the compact star. If one makes this assumption and uses the fact that the system is seen almost edge-on, it turns out that with a mass of the F-star of ~ 1.0 to $1.5M_{\odot}$, the mass of the compact star works out to be $> 6M_{\odot}$. These authors therefore conclude that the compact object in the system is, in all likelihood, a black hole.

However, there are clear arguments against such an interpretation, as follows.

If the He II 4686 line indeed arises in the disk, as Cowley et al. assume, then its strength should go down during the primary eclipse (when the disk is eclipsed). However, according to Cowley et al.’s (1990) measurements (their table), the equivalent width W_{λ} of the line goes up by a factor 2 to 3 during primary eclipse ($W_{\lambda} \approx 10$ – 17 Å during primary eclipse, compared to 6–8 Å outside eclipse). Since W_{λ} is defined with respect to the height of the continuum, this means that while the continuum of the disk goes down by more than a factor 2 to 3 during primary eclipse (when the disk is maximally eclipsed) the flux of the He II 4686 line received on Earth hardly changes, i.e. the real strength of the line does not change.

This can only imply that the line-emitting region is hardly eclipsed when the disk is almost completely eclipsed.

The He II 4686 line must therefore be formed in a region that extends far outside the limits of the disk. In Of-stars and Wolf-Rayet stars this line typically arises in a wind, and the large observed width represents the outflow velocity of the wind.

The large extent of the line-emitting region in CAL 87 makes it likely that also here this line arises in an extended wind or corona.

In view of the proximity of the strong X-ray source to the stellar surface, the side of the star facing the source will be strongly heated [arguments given under (c)]. This heating is also likely to drive a wind from the heated side of the star [e.g. see Tavani et al. (1989)].

The part of the He II 4686 line arising in the wind from this heated side will certainly not produce a radial velocity representative of the compact star.

One therefore expects the mean radial velocity measured for the He II 4686 line to be some weighted mean of the radial velocity

of the winds from the heated side of the companion and of the disk. As long as this “weighted mean” velocity resulting in this way mimics the velocity of a point situated between the center of mass of the system and the compact star, the He II 4686-line “radial velocity curve” will show the correct phase relation with respect to the photometric curve (i.e. maximum radial velocity at phase 0.75) as is observed.

However, the *velocity amplitude* K in that case will by no means be that of the compact star. It will correspond to the above-mentioned unknown “weighted mean” point in the system.

In view of the above, the radial velocity amplitude of the He II 4686 line is not expected to yield useful information about the mass function of the system, nor about the masses of the components. This makes the evidence for a black hole in the system no longer compelling.

Moreover, the X-ray spectrum of the source in no way resembles that of the known X-ray binary black hole candidates. Although the X-ray spectra of these sources are somewhat softer than those of accreting neutron stars, the black hole sources still emit the bulk of their X-ray flux in the spectral range 0.5–20 keV (cf. McClintock 1979), where the soft sources CAL 83 and 87 emit hardly anything at all.

No theoretical model of an accreting black hole is known that can produce an X-ray source spectrum that peaks in the range 30–50 eV and has the observed X-ray luminosity in the range 10^{37} – 10^{38} erg s $^{-1}$.

5.2.3. Summary

- The eclipsing binary lightcurve of the CAL 87 system indicates that it consists of a bright accretion disk and a much fainter normal F-G star with a mass ~ 1.4 – $1.5M_{\odot}$.
- The companion shows a large heating effect, as evidenced by the depth of the secondary eclipse; the X-ray heated side is at least some 3 times brighter than the non-heated side of the star.
- The He II 4686 line arises in a region much larger than the disk and its radial velocity amplitude yields no useful information on the mass of the compact component of the system.

5.3. The CAL 83 system

The optical and X-ray brightness of this system are considerably larger than those of CAL 87 and its optical lightcurve is totally different from that of the latter system. The lightcurve has a sine-wave shape with an amplitude of only 0.11 m in V . The mean magnitude observed in December 1984 is 16.86, making Cal 83 optically some 2 m1 brighter than CAL 87 at maximum brightness (Smale et al. 1988). The orbital period is $1^d.0436 \pm 0^d.0044$. With this period the companion is either an (evolved) main-sequence star of mass $\gtrsim 2M_{\odot}$, or a post-main-sequence (subgiant) star of lower mass. A $1M_{\odot}$ subgiant would only be able to drive mass transfer on a nuclear time scale, at a rate not exceeding $\sim 10^{-9}M_{\odot}$ yr $^{-1}$ (Pylyser & Savonije 1988, 1989). This is insufficient by a factor 100 to power an accreting white dwarf that is burning hydrogen to an integrated X-ray luminosity of $\gtrsim 10^{38}$ erg s $^{-1}$. For a neutron star it is insufficient by a factor 10. On the other hand, if one assumes the companion to be the more massive star in the system, it will transfer mass on its (much shorter) thermal timescale. A star of mass $\gtrsim 1.5M_{\odot}$ will in this

way drive a mass-transfer rate $\gtrsim 10^{-7} M_{\odot} \text{ yr}^{-1}$, sufficient to turn a white dwarf into an $\gtrsim 4 \cdot 10^{37} \text{ erg s}^{-1}$ X-ray source.

One expects the accretion disk in the system to be an important light source, as is the case for the CAL 87 system.

Since no eclipses are observed, the disk in CAL 83 is expected to be seen much more nearly “face-on” than the disk in CAL 87 (which is seen almost edge-on). The large observed disk area will then contribute to a larger optical luminosity from the disk in CAL 83. Assuming that CAL 87 has $\cos i \leq 0.2$, since deep eclipses are observed, and that for CAL 83 $\cos i > 0.45$ (since no eclipses are observed and the ratio of the Roche lobe radius of the companion star to the orbital radius $R_1/a \sim 0.45$, see below), the disk in CAL 83 will have ~ 7 times larger projected area than the disk in CAL 87 (a factor 2.2 due to the different inclination and a factor 3.2 due to the larger dimensions of the CAL 83 system). Assuming both disks to have roughly the same average surface brightness, one would expect the disk in CAL 83 to be some 7 times (= 2.1 mag) brighter than the one in CAL 87.

This would already account for the entire magnitude difference between the Cal 83 and CAL 87 systems ($16^{\text{m}}86$ and 18.9^{m} , respectively). The sinusoidal lightcurve of the system is just what one expects in the case of one-sided X-ray heating of the stellar surface in a system seen at low inclination, such that no eclipses occur.

In such a system the disk will always be visible, and will be a (strong) constant lightsource next to the star.

It is easy to show that in the case of one-sided heating which produces a surface brightness f_1 on the heated side, while the undisturbed surface brightness of the dark side of the star is f_0 , the lightcurve of the star viewed at an orbital inclination i will have the shape

$$F = [(f_1 + f_0) + (f_1 - f_0) \sin i \cos \omega t] / 2 \quad (3)$$

where $\omega = 2\pi/P$, and P is the orbital period. Expressing the optical luminosity L_d of the disk in terms of the mean observed luminosity $[(f_1 + f_0)/2f_0] L_s$ of the companion star yields:

$$L_d = \frac{\alpha(f_1 + f_0)}{2f_0} L_s \quad (4)$$

where L_s is the luminosity of the unheated star. Then the total optical luminosity of the system can be written as

$$\left[(1 + \alpha) \frac{f_1 + f_0}{2f_0} + \frac{f_1 - f_0}{2f_0} \sin i \cos 2\omega t \right] L_s. \quad (5)$$

Therefore, the 0.11^{m} sinusoidal modulation in the brightness of CAL 83 yields

$$\frac{(f_1 - f_0) \sin i}{(1 + \alpha)(f_1 + f_0)} = 0.11 \quad (6)$$

(since $0^{\text{m}}11$ corresponds to $\sim 11\%$). The absence of eclipses indicates that $\cos i > 0.45$ or $\sin i < 0.9$. We shall attempt below to estimate α and f_1/f_0 from the observed characteristics of the system. We will assume, for the sake of argument, that the factor of ~ 4 difference in X-ray luminosity between Cal 83 and Cal 87 is real and not influenced by observational uncertainties.

Such a ~ 4 times larger observed X-ray luminosity of CAL 83 with respect to CAL 87 may be due to:

(i) a more evolved companion [since at the same companion mass, \dot{M} is about 1.5 times larger for a companion at turn-off than on the zero-age main sequence (see Fig. 2)];

(ii) a more massive companion;

(iii) a different orbital inclination (at a high inclination, such as that of CAL 87, the X-ray source may be partly obscured).

We expect that the third mentioned effect does not play a major role here, since the X-ray luminosity *observed* for CAL 87 is $\sim 4 \cdot 10^{37} \text{ erg s}^{-1}$, which fits very well with the mass-transfer rate expected from its 1.4 to $1.5 M_{\odot}$ companion (see Fig. 2).

Assuming that the more evolved status (because of the wider orbit) of the companion of Cal 83 may contribute a factor 1.5 to its larger mass-transfer rate, we conclude that the remaining factor of 2.7 could imply a companion mass that is 1.4 times larger than in the case of Cal 83 (i.e. 1.9 to $2.0 M_{\odot}$). At the distance of the LMC the intrinsic (unheated-side) magnitude of such a star is $V \sim 20^{\text{m}}$, which is negligible with respect to the $16^{\text{m}}86$ of the accretion disk. Only the heated side may possibly contribute to the total system luminosity. Assuming the same heating efficiency as in CAL 87, one expects the heated side of the companion to CAL 83 to be some 3 times brighter than the heated side of CAL 87's companion (due to the 3 times larger surface area; the X-ray flux at the surface of the companion is about the same in both systems), corresponding to an apparent magnitude in the LMC of $V = 18^{\text{m}}4$ (we assume that the heated side of the donor contributes less than half the total system luminosity in CAL 87), i.e. at least some 4 times fainter than the accretion disk of CAL 83. So, the disk provides 80 percent or more of the optical luminosity of the system. With Eqs. (4) and (6) this yields $\alpha \geq 2.3$ and $f_1 > 2.5 f_0$, implying indeed a considerable heating effect [$\sin i < 0.9$ was used in Eq. (6)]. In turn, this large heating effect on the companion of Cal 83 makes it plausible that also the companion of Cal 87 shows a large heating effect, i.e. that the secondary eclipse in that system is primarily due to the eclipse of the heated side of the companion.

6. The expected formation rate and incidence of supersoft binary X-ray sources in the Galaxy

Systems of this type are expected to be the outcome of common-envelope (CE) evolution of initially fairly wide binaries consisting of a red giant with a degenerate core of mass 0.7 to $1.2 M_{\odot}$ and a main-sequence star of mass 1.5 – $2.0 M_{\odot}$ (cf. Paczynski 1976; Meyer & Meyer-Hofmeister 1979; Webbink 1984; Iben & Tutukov 1984; Taam & Bodenheimer 1989). During the CE phase the main-sequence star spirals down into the envelope of the red giant, causing the latter to be ejected. In the end a short-period system results, consisting of the massive white dwarf and the main-sequence star. In view of the short duration of the spiral-in process the latter star will not have accreted a significant amount of mass during this phase.

From the initial-mass-final-mass relation derived by Weidemann (1987) we find that in order to produce a $0.7 M_{\odot}$ white dwarf the initial stellar mass must be $4 M_{\odot}$, a $0.8 M_{\odot}$ white dwarf requires an initial mass of $6 M_{\odot}$, and a $1.2 M_{\odot}$ white dwarf needs an initial mass of $8 M_{\odot}$. The number of systems that go through this evolution and produce binaries with $P \sim 8^{\text{h}}$ to 1 day of the type required here can be estimated as follows.

The fraction f of all systems in a certain mass range of the primary stars that go through this evolution is:

$$f = \int_{a_1}^{a_2} F(\log a) d \log a \int_{q_1}^{q_2} G(q) dq \quad (7)$$

where $F(\log a)$ is the distribution function of the logarithm of orbital radii a of unevolved binaries; $G(q)$ is the distribution of

mass ratios of unevolved binaries ($q \equiv M_2/M_1$, M_2 being the less massive component of the original binary); (a_1, a_2) is the range of initial orbital radii that is required to produce post-spiral-in systems with $P \simeq 8^h-24^h$; and (q_1, q_2) is the required range of initial mass ratios of secondary and primary in pre-spiral-in systems.

The required intervals in these parameters and their distribution functions will now be discussed.

6.1. Orbital radii (semi-major axes) a

We will assume circular orbits.

The range in required post-spiral-in orbital radii is about a factor of two (corresponding an interval in the orbital period 8^h-24^h). Spiral-in calculations (Webbink 1984) show that for a given initial primary mass M_1 and a mass ratio q , the ratio of initial and final orbital radii is a fixed quantity. This implies that also the range in the initial orbital radii was a factor of two, corresponding to a range of 0.3 in $\log a$.

Since $F(\log a)$ is approximately constant for a between 10^{-2} and 10^4 AU (Kraicheva et al. 1978), one has that initial $\log a$ values in a range 0.3 make up a fraction 0.3/6 of all binaries, i.e. $\int_{a_1}^{a_2} F(\log a) d \log a = 0.05$.

6.2. The initial mass-ratio distribution of unevolved binaries

This distribution is not very well established, especially for low values of q . However, there is general agreement (see e.g. Halbwachs 1987; Hogeveen 1990) that the distribution increases towards lower q values, although the slope of $G(q)$ is not yet well established. As a conservative assumption we will adopt a flat distribution: $G(q)=1$ for $0 \leq q \leq 1$. We will adopt an average initial primary mass $M_1=6M_\odot$ which, with $M_2=1.5$ to $2.0M_\odot$, yields an initial q -range of $q_1=0.25$ to $q_2=0.33$, yielding

$$\int_{q_1}^{q_2} G(q) dq = 0.08.$$

Furthermore, for the fraction of stars that are in binaries, B , we (conservatively) assume $B=0.5$ (see e.g. Abt 1983). Combining the above quantities we obtain in Eq. (7):

$$Bf = B \int_{a_1}^{a_2} F(\log a) d \log a \int_{q_1}^{q_2} G(q) dq = 0.002. \quad (8)$$

Taking Miller & Scalo's (1979) initial mass function $\psi(M)$ one finds that the stellar birth rate in the galactic disk for masses in the M_1 -range $4M_\odot$ to $8M_\odot$ is $3.64 \cdot 10^{-2} \text{ yr}^{-1}$ while that for masses in the range $6M_\odot$ to $8M_\odot$ is $1.1 \cdot 10^{-2} \text{ yr}^{-1}$.

The galactic formation rate of close binaries consisting of a massive white dwarf and a $1.5-2.0M_\odot$ main-sequence star, originating from the appropriate intervals of initial primary masses, are listed in Table 1. The table also lists the expected numbers of ultrasoft binary X-ray sources resulting from these initial primary masses intervals, for the Galaxy as well as the LMC.

An average accretion lifetime τ_x of $\sim 5 \cdot 10^6$ yr was adopted, since after accretion of $\sim 0.7M_\odot$ (about half of the envelope of the $1.5-2.0M_\odot$ star) the white dwarf will either have undergone a carbon-deflagration or have collapsed to a neutron star.

In view of the uncertainties in the IMF, the expected X-ray lifetimes, etc. the uncertainties in the numbers in the table are at least a factor of two.

Table 1. The formation rate of close binaries consisting of a massive white dwarf and a $1.5-2.0M_\odot$ main-sequence star, and the expected Galactic and LMC numbers of accreting white dwarf systems. The uncertainties in the numbers are at least a factor two. The numbers for the LMC are obtained by assuming the mass of LMC to be 1/5th that of the Galaxy

	$M_1=4-8M_\odot$ ($M_{\text{w.d.}}=0.7-1.2M_\odot$)	$M_1=6-8M_\odot$ ($M_{\text{w.d.}}=0.8-1.2M_\odot$)
Galactic formation rate	$7.2 \cdot 10^{-5} \text{ yr}^{-1}$	$2.2 \cdot 10^{-5} \text{ yr}^{-1}$
Expected Galactic number ($\tau_x = 5 \cdot 10^6 \text{ yr}$)	360	110
Expected LMC number (idem)	72	22

Comparison with the observations is only possible for the LMC: here two ultrasoft sources were detected when less than twenty percent of the LMC was deeply surveyed. Therefore, there may well be about a dozen such sources in the LMC. Such a number would, according to Table 1, fit well with an origin from systems with primary stars in the mass range $6-8M_\odot$ (white dwarf masses $0.8-1.2M_\odot$), but possibly not with an origin from systems with primary stars in the $4-6M_\odot$ range. This finding seems to imply that a white dwarf mass of at least $0.8M_\odot$ may be required to produce an ultrasoft X-ray source.

We thus conclude – adopting the accreting white dwarf model – that the incidence of ultrasoft sources in the LMC indicates that the progenitors of the white dwarfs were stars in the mass range $6-8M_\odot$. From this we estimate that some 110 such sources are expected to be present in the Galactic disk. Adopting a disk radius of 13 kpc, the nearest such source is expected to be situated at a distance ~ 2 kpc from us. Therefore, if these sources are located in the galactic plane, almost all of their soft X-ray flux would be absorbed in the interstellar medium, and they would not be detectable.

6.3. Comparison: the expected incidence of Her X-1 and post Her X-1 binaries in the Galaxy

Such systems are expected to have resulted from a spiral-in scenario similar to the one described above, but with more massive red giants in the mass range $8-15M_\odot$ (Sutantyo 1975; Verbunt et al. 1990), such that after spiral-in the remnant core of the red giant was massive enough to collapse to a neutron star. In this case one will have to add in Eq. (7) the survival probability P of the systems after the supernova explosion.

Carrying out a similar calculation as above, we obtain a formation rate of Her X-1 like systems of

$$R \approx 2.2 \cdot 10^{-5} P \text{ yr}^{-1}.$$

Adopting a survival probability of 0.3 (see e.g. Sutantyo 1991) one expects a galactic formation rate of $0.7 \cdot 10^{-5} \text{ yr}^{-1}$.

The duration of the X-ray phase in Her X-1 like systems (with stable mass transfer) is relatively short, of order $(1-5) \cdot 10^5 \text{ yr}$

(Savonije 1983), resulting in an expected galactic number of Her X-1 like systems of between 0.7 and 3.5, i.e. 2 ± 1.5 at any time.

Although this expected incidence is low, it fits well with the observed rareness of Her X-1 like binaries. The low incidence is, of course, due to the very short duration of the X-ray binary phase in these systems, some 10^2 – 10^3 times shorter than in the “standard” low-mass X-ray binaries.

Similar to the white-dwarf systems, the Her X-1 like systems must also go through a longer-lasting ($\sim 10^7$ yr) phase with a large mass-transfer rate, of order $10^{-7} M_{\odot} \text{ yr}^{-1}$. From the above formation rate one would expect some 70 systems of this type in the Galaxy. It is at present totally unclear what such systems – which should be at relatively large distances from the galactic plane in view of the large kick velocity received during their supernova event – will look like. In any case, it seems highly unlikely that they would resemble the ultrasoft ROSAT sources, since at these high Z -values these sources would most probably already have been found in earlier X-ray surveys.

7. Conclusions

(a) For a limited range of mass transfer rates, between $\sim 10^{-7}$ and $4 \cdot 10^{-7} M_{\odot} \text{ yr}^{-1}$, massive (0.7 – $1.2 M_{\odot}$) white dwarfs will be in a phase of stable hydrogen burning without a substantial increase in radius.

(b) Such white dwarfs are expected to appear as near-Eddington limited (0.4 to $1.0 L_{\text{Edd}}$) ultra-soft X-ray sources, with peak energy fluxes 30 – 50 eV – as observed for the ultrasoft ROSAT LMC sources CAL 83 and RXJ 0527.8–6954.

(c) The required mass accretion rates can, in short period ($\lesssim 1$ – 2^{d}) binaries, only be supplied by companion stars in the mass-range 1.4 – $2.2 M_{\odot}$.

(d) An analysis of the optical and X-ray characteristics of the systems of CAL 87 and CAL 83 shows that these characteristics are consistent with the presence in these systems of companions just in the required mass range having masses of 1.4 – $1.5 M_{\odot}$ and 1.9 – $2.1 M_{\odot}$, respectively.

(e) The observed incidence of ultrasoft sources in the LMC, together with their calculated birthrate suggests that the progenitor stars of their white dwarfs were stars in the mass range 6 – $8 M_{\odot}$. The number of sources expected in the galaxy from binary evolution with primary stars in this mass range is ~ 130 .

Acknowledgements. We thank J. Grindlay and H. Spruit for discussions, and J. Greiner for sharing unpublished data with us. This research was supported in part by the National Science Foundation under Grant No. PHY89-04035.

References

- Abt H.A., 1983, ARA&A 21, 343
 Bradt H.V., McClintock J.E., 1983, ARA&A 21, 13
 Callanan P.J., Machin G., Naylor T., Charles P.A., 1989, MNRAS 241, 37
 Cowley A.P., Schmidtke P.C., Crampton D., Hutchings J.B., 1990, ApJ 350, 288
 Giacconi R., 1975, in: Proc. of the 7th Texas Conf. on Relativistic Astrophysics, Ann N.Y., Acad. Sci. 262, 312
 Greiner J., Hasinger G., Kahabka P., 1991, A&A 246, L17
 Halbwachs J.L., 1987, A&A 183, 234
 Hatchett S., McCray R., 1977, ApJ 211, 552
 Hogeveen S., 1990, Ap&SS 173, 315
 Iben I., Tutukov A.V., 1984, ApJS 54, 335
 Kraicheva Z.F., Popova E.I., Tutukov A.V., Yungelson L.R., 1978, in: Żytkow A. (ed.) Non-stationary Evolution of Close Binaries. Polish Science Publishers, Warszawa, p. 25
 Levine A., Rappaport S., Putney A., Corbet R., Nagase F., 1991, ApJ 381, 101
 Long K.S., Helfand D.J., Grabelsky D.A., 1981, ApJ 248, 925
 McClintock J.E., 1989, in: Ögelman H., van den Heuvel E.P.J. (eds.) Timing Neutron Stars. Kluwer, Dordrecht, p. 209
 McClintock J.E., Remillard R.A., Margon B., 1981, ApJ 243, 900
 Meyer F., Meyer-Hofmeister E., 1979, A&A 78, 167
 Miller G.E., Scalo J.M., 1979, ApJS 41, 513
 Naylor T., Callanan P.J., Machin G., Charles P.A., 1989, IAU Circ. No 4747
 Nomoto K., 1982, ApJ 253, 798
 Nomoto K., Nariai K., Sugimoto D., 1979, PASJ 31, 287
 Paczyński B., 1971, ARA&A 9, 183
 Paczyński B., 1976, in: Eggleton P.P. et al. (eds.) Structure and Evolution of Close Binary Stars. Reidel, Dordrecht, p. 75
 Paczyński B., Żytkow A.N., 1978, ApJ 222, 604
 Pakull M.W., Beuermann K., van der Klis M., van Paradijs J., 1988, A&A 203, L27
 Pylyser E.H.P., Savonije G.J., 1988, A&A 191, 57
 Pylyser E.H.P., Savonije G.J., 1989, A&A 208, 52
 Savonije G.J., 1983, in: Lewin W.H.G., van den Heuvel E.P.J. (eds.) Accretion-driven Stellar X-ray Sources. Cambridge University Press, Cambridge, p. 343
 Sienkiewicz R., 1980, A&A 85, 295
 Sion E.M., Acierno M.J., Tomczyk S., 1979, ApJ 230, 832
 Smale A.P., Corbet R.H.D., Charles P.A., Ilovaisky S.A., Mason K.O., Motch C., Mukui K., Naylor T., Parmar A.N., van der Klis M., van Paradijs J., 1988, MNRAS 233, 51
 Sutantyo W., 1975, A&A 41, 47
 Sutantyo W., 1991, in: van den Heuvel E.P.J., Rappaport S.A. (eds.) X-ray Binaries and the Formation of Binary and millisecond Radio Pulsars. Kluwer, Dordrecht (in press)
 Taam R.E., Bodenheimer P., 1989, ApJ 337, 849
 Tavani M., Ruderman M.A., Shaham J., 1989, ApJ 342, L31
 Trümper J., Hasinger G., Aschenbach B., Bräuninger H., Briel U.G., Burkert W., Fink H., Pfefferman E., Pietsch W., Predehl P., Schmitt J.H.M.M., Voges W., Zimmerman U., Beuermann K., 1991, Nat 349, 579
 van Paradijs J., 1983, in: Lewin W.H.G., van den Heuvel E.P.J. (eds.) Accretion-driven Stellar X-ray Sources. Cambridge University Press, Cambridge, p. 189
 Verbunt F., Wijers R.A.M.J., Burm H., 1990, A&A 234, 195
 Webbink R.F., 1984, ApJ 277, 355
 Weidemann V., 1987, A&A 188, 74